Role of different types of subsystems in a doubly driven Λ system in ^{87}Rb

Kanhaiya Pandey*

Centre for Quantum Technologies, National University of Singapore, 3 Science Drive 2, Singapore 117543

(Received 30 October 2012; revised manuscript received 10 March 2013; published 26 April 2013)

The well-known Λ system using two ground-state hyperfine levels, $F_g = 1$ and $F_g = 2$ of $5S_{1/2}$, and one hyperfine level, $F_e = 2$ of excited state of $5P_{3/2}$ of ^{87}Rb, has been recently studied using two counterpropagating control lasers [Sapam Ranjita Chanu, Kanhaiya Pandey, and Vasant Natarajan, Europhys. Lett. **98**, 44009 (2012)]. The experiment shows conversion of electromagnetically induced transparency into electromagnetically induced absorption because the doubly driven Λ system forms various subsystems. We here present a detailed theoretical study of the different possible subsystems created by this configuration. We also explore the possibility of tuning the strength of individual subsystems by changing the polarization of the control lasers.

DOI: 10.1103/PhysRevA.87.043838 PACS number(s): 42.50.Gy, 42.50.Hz, 32.80.Qk

I. INTRODUCTION

Laser-induced coherence between levels in the multilevel systems is the core of all the quantum interference effects in near-resonant laser-atom interaction. This laser-induced coherence is also known as transfer of coherence (TOC), since simultaneous driving of different levels with lasers induces coherence between the levels which are not directly driven. The TOC gives rise to interesting phenomenons like electromagnetically induced transparency (EIT) [1], electromagnetically induced absorption (EIA), and coherent population trapping (CPT). EIT is an example of suppressing the absorption of a probe laser in the presence of a control laser in the three-level systems (Λ, V, and Ξ) due to TOC between levels which are not allowed by dipole transition. EIT has been extensively studied due to its potential application in a wide variety of fields such as lasing without inversion [1,2], high-resolution spectroscopy [3,4], enhancement of second- and third-order nonlinear processes [5], polarization control [6,7], and storage of light [8].

The modification of the probe laser absorption due to TOC has been investigated beyond the three-level system [9–15]. Splitting and reshaping of the EIT peak has been studied using two counterpropagating control lasers having the same polarization to form a standing wave [16–18]. The EIT has also been extensively studied in consideration of multilevel systems and different polarizations of the control and probe lasers in vapor [19–23] as well as in cold atoms [24–26]. The effect of the excited hyperfine levels on the Λ system has also been studied [27]. In the presence of a magnetic field, splitting and reduction of the linewidth of the EIT have been studied as well [28,29].

The previously studied Λ system using $F = 1 \rightarrow F = 2 \leftrightarrow F = 2$, in ^{87}Rb atom including all the magnetic sublevels is described based on the numerical analysis [28–30]. Here we analytically describe the Λ system, $F = 1 \rightarrow F = 2 \leftrightarrow F = 2$ with two counterpropagating control lasers (a doubly driven Λ system) having orthogonal polarization in ^{87}Rb vapor. We identify all the subsystems and the role of individual subsystems and coherence for this doubly driven Λ system. We also show under what conditions the effects of individual subsystems and coherence will dominate and how one subsystem influences others.

In order to address this problem we first discuss a generalized N-level system of a particular kind, as shown in Fig. 1, and investigate the role of different kinds of coherence. Then we discuss a three-level Λ system, a four-level N system, a five-level M system, and a six-level NN system, since these types of systems act as the subsystems for the doubly driven Λ system. Furthermore, we also discuss the effect of Doppler averaging for these systems. Finally we describe the role of subsystems formed by a doubly driven Λ system in ^{87}Rb.

II. THEORETICAL FORMULATION

The Hamiltonian of the general N-level system of the type shown in Fig. 1 in the rotating frame with rotating wave approximation (RWA) is given as

$$H = \hbar \sum_{j=1}^{N-1} \frac{\Omega_{j,j+1}}{2} |j\rangle\langle j+1| + \text{H.c.} + 0|1\rangle\langle 1| + \hbar \sum_{j=2}^{N} \sum_{i=2}^{j} (-1)^i \Delta_{i-1,i} |j\rangle\langle j|, \quad (1)$$

where $\Omega_{j,j+1}$ and $\Delta_{j,j+1}$ are the Rabi frequency and the detuning of the lasers driving levels $|j\rangle \leftrightarrow |j+1\rangle$. In the above Hamiltonian the first summation contains off-diagonal terms and is about interaction between the adjacent levels with strength (Rabi frequency) of $\Omega_{12}, \Omega_{23}, \ldots, \Omega_{N-1N}$. The second summation contains the diagonal terms which are the energies of various levels in the rotating frame. For example, the energy of the jth level is $\Delta_{12} - \Delta_{23} + \Delta_{34} - \Delta_{45} \cdots (-1)^j \Delta_{j-1j}$. The energy of the ground state $|1\rangle$ is taken to be zero. The probe laser is driving the levels $|1\rangle$ and $|2\rangle$ while the control lasers are driving $|2\rangle \leftrightarrow |3\rangle \leftrightarrow |4\rangle \leftrightarrow \cdots \leftrightarrow |N\rangle$. The populations in the various levels and coherence between them is described by the density matrix ρ. The diagonal terms of the density matrix describe the population while the off-diagonal terms describe the coherences. The time evolution of the density matrix is given by the optical Bloch equation (OBE) [31], which is

$$i\hbar \frac{d\rho}{dt} = [H, \rho]. \quad (2)$$

*kanhaiyapandey@gmail.com

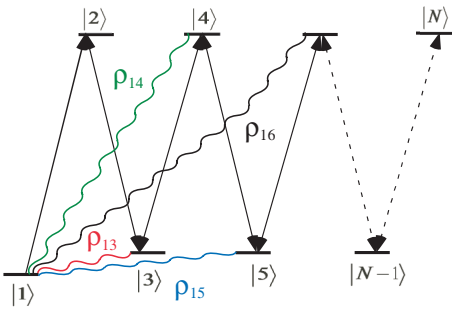

FIG. 1. (Color online) The energy-level diagram for an N-level system. The light-induced coherence or transfer of coherence (TOC) between various levels is shown by the wavy lines.

Time evolution of the population in the various levels is given as

$$\begin{aligned}
\dot{\rho}_{11} &= -\Gamma_1\rho_{11} + \sum_{i=2}^{N}\Gamma_{i1}\rho_{ii} + \frac{i}{2}\Omega_{12}^{*}\rho_{12} - \frac{i}{2}\Omega_{12}\rho_{21},\\
\dot{\rho}_{22} &= -\Gamma_2\rho_{22} + \sum_{i=1,i\neq 2}^{N}\Gamma_{i2}\rho_{ii} + \frac{i}{2}\Omega_{12}\rho_{21} - \frac{i}{2}\Omega_{12}^{*}\rho_{12}\\
&\quad + \frac{i}{2}\Omega_{23}^{*}\rho_{23} - \frac{i}{2}\Omega_{23}\rho_{32},\\
&\vdots\\
\dot{\rho}_{jj} &= -\Gamma_j\rho_{jj} + \sum_{i=1,i\neq j}^{N}\Gamma_{ij}\rho_{ii} + \frac{i}{2}\Omega_{j-1j}\rho_{jj-1},\\
&\quad - \frac{i}{2}\Omega_{j-1j}^{*}\rho_{j-1j} + \frac{i}{2}\Omega_{jj+1}^{*}\rho_{jj+1} - \frac{i}{2}\Omega_{jj+1}\rho_{j+1j},\\
&\vdots\\
\dot{\rho}_{NN} &= -\Gamma_N\rho_{NN} + \sum_{i=1,i\neq N}^{N}\Gamma_{iN}\rho_{ii} + \frac{i}{2}\Omega_{N-1N}^{*}\rho_{N-1N}\\
&\quad - \frac{i}{2}\Omega_{N-1N}\rho_{NN-1},
\end{aligned} \tag{3}$$

where Γ_{ij} is the spontaneous decay rate of level $|i\rangle$ into level $|j\rangle$. For the nonzero value of Γ_{ij} the energy of level $|i\rangle$ has to be higher than that of level $|j\rangle$. Furthermore, the value of Γ_{ij} is determined by the dipole matrix element between levels $|i\rangle$ and $|j\rangle$. The $\Gamma_i(=\sum_{j=1,j\neq i}^{N}\Gamma_{ij})$ is the total decay rate of level $|i\rangle$.

The time evolution of the coherence between level $|1\rangle$ and various other levels is given as

$$\begin{aligned}
\dot{\rho}_{12} &= -\left[\frac{\Gamma_1+\Gamma_2}{2} - i\Delta_{12}\right]\rho_{12} + \frac{i}{2}\Omega_{12}(\rho_{11}-\rho_{22})\\
&\quad + \frac{i}{2}\Omega_{23}^{*}\rho_{13},\\
\dot{\rho}_{13} &= -\left[\frac{\Gamma_1+\Gamma_3}{2} - i\left(\Delta_{12}-\Delta_{23}\right)\right]\rho_{13} - \frac{i}{2}\Omega_{12}\rho_{23}\\
&\quad + \frac{i}{2}\Omega_{23}\rho_{12} + \frac{i}{2}\Omega_{34}^{*}\rho_{14},\\
&\vdots
\end{aligned}$$

$$\begin{aligned}
\dot{\rho}_{1N-1} &= -\left[\frac{\Gamma_1+\Gamma_{N-1}}{2} - i\left(\sum_{i=2}^{N-1}(-1)^i\Delta_{i-1,i}\right)\right]\rho_{1N-1}\\
&\quad - \frac{i}{2}\Omega_{12}\rho_{2N-1} + \frac{i}{2}\Omega_{N-2N-1}\rho_{1N-2} + \frac{i}{2}\Omega_{N-1N}^{*}\rho_{1N},\\
\dot{\rho}_{1N} &= -\left[\frac{\Gamma_1+\Gamma_N}{2} - i\left(\sum_{i=2}^{N}(-1)^i\Delta_{i-1,i}\right)\right]\rho_{1N}\\
&\quad - \frac{i}{2}\Omega_{12}\rho_{2N} + \frac{i}{2}\Omega_{N-1N}\rho_{1N-1}.
\end{aligned} \tag{4}$$

In the steady state $\dot{\rho}_{ij}=0$ for all i and j. In the case of a weak probe limit, $\Omega_{12}\rho_{23}$, $\Omega_{12}\rho_{24},\ldots,\Omega_{12}\rho_{2N}\approx 0$ and $\rho_{22}\approx 0$.

The set of Eqs. (4) with the aforementioned approximation gives the following:

$$\rho_{1N} \approx \frac{i}{2}\frac{\Omega_{N-1N}}{\gamma_{1N}}\rho_{1N-1}, \tag{5}$$

$$\rho_{1N-1} \approx \frac{i}{2}\frac{\Omega_{N-2N-1}}{\gamma_{1N-1}}\rho_{1N-2} + \frac{i}{2}\frac{\Omega_{N-1N}^{*}}{\gamma_{1N-1}}\rho_{1N}, \tag{6}$$

where the general form of

$$\gamma_{1j} = \frac{\Gamma_1+\Gamma_j}{2} - i\sum_{i=1}^{j-1}(-1)^{i+1}\Delta_{i,i+1}. \tag{7}$$

For example, $\gamma_{12}=\frac{\Gamma_1+\Gamma_2}{2}-i\Delta_{12}$, $\gamma_{13}=\frac{\Gamma_1+\Gamma_3}{2}-i(\Delta_{12}-\Delta_{23})$, $\gamma_{14}=\frac{\Gamma_1+\Gamma_4}{2}-i(\Delta_{12}-\Delta_{23}+\Delta_{34})$, $\gamma_{15}=\frac{\Gamma_1+\Gamma_5}{2}-i(\Delta_{12}-\Delta_{23}+\Delta_{34}-\Delta_{45})$, and so on.

Equations (5) and (6) produce

$$\rho_{1N-1} = \frac{\frac{i}{2}\frac{\Omega_{N-2N-1}}{\gamma_{1N-1}}}{1+\frac{1}{4}\frac{|\Omega_{N-1N}|^2}{\gamma_{1N}\gamma_{1N-1}}}\rho_{1N-2}. \tag{8}$$

Again from Eq. (4),

$$\rho_{1N-2} \approx \frac{i}{2}\frac{\Omega_{N-3N-2}}{\gamma_{1N-2}}\rho_{1N-3} + \frac{i}{2}\frac{\Omega_{N-2N-1}^{*}}{\gamma_{1N-2}}\rho_{1N-1}. \tag{9}$$

From Eqs. (8) and (9),

$$\rho_{1N-2} = \frac{\frac{i}{2}\frac{\Omega_{N-3N-2}}{\gamma_{1N-2}}}{1+\frac{\frac{1}{4}\frac{|\Omega_{N-2N-1}|^2}{\gamma_{1N-2}\gamma_{1N-1}}}{1+\frac{1}{4}\frac{|\Omega_{N-1N}|^2}{\gamma_{1N-1}\gamma_{1N}}}}\rho_{1N-3}. \tag{10}$$

From the above general formula we can write

$$\rho_{13} = \frac{\frac{i}{2}\frac{\Omega_{23}}{\gamma_{13}}}{1+\frac{\frac{1}{4}\frac{|\Omega_{34}|^2}{\gamma_{13}\gamma_{14}}}{1+\frac{\frac{1}{4}\frac{|\Omega_{45}|^2}{\gamma_{14}\gamma_{15}}}{1+\frac{\frac{1}{4}\frac{|\Omega_{56}|^2}{\gamma_{15}\gamma_{16}}}{1+\frac{\cdot}{1+\frac{\cdot}{1+\frac{1}{4}\frac{|\Omega_{N-1N}|^2}{\gamma_{1N-1}\gamma_{1N}}}}}}}} \tag{11}$$

Again from Eq. (4) in steady state

$$\rho_{12} \approx \frac{i}{2}\frac{\Omega_{12}}{\gamma_{12}}\rho_{11} + \frac{i}{2}\frac{\Omega_{23}^{*}}{\gamma_{12}}\rho_{13}. \tag{12}$$

Equations (11) and (12) give

$$\rho_{12} = \frac{\frac{i}{2}\frac{\Omega_{12}}{\gamma_{12}}\rho_{11}}{1 + \cfrac{\frac{1}{4}\frac{|\Omega_{23}|^2}{\gamma_{12}\gamma_{13}}}{1 + \cfrac{\frac{1}{4}\frac{|\Omega_{34}|^2}{\gamma_{13}\gamma_{14}}}{1 + \cfrac{\frac{1}{4}\frac{|\Omega_{45}|^2}{\gamma_{14}\gamma_{15}}}{1 + \cfrac{\frac{1}{4}\frac{|\Omega_{56}|^2}{\gamma_{15}\gamma_{16}}}{1 + \cfrac{\cdot}{1 + \cfrac{\cdot}{1 + \frac{1}{4}\frac{|\Omega_{N-1N}|^2}{\gamma_{1N-1}\gamma_{1N}}}}}}}}}. \tag{13}$$

The imaginary part of ρ_{12}, $\mathrm{Im}(\rho_{12})$, represents the absorption of the probe laser while the real part represents the dispersion.

In the regime of the weak probe, for the system shown in Fig. 1, all the population will be pumped to state $|1\rangle$, i.e., $\rho_{11} \approx 1$. But for the more complex system the population might be distributed to other ground states. In that case ρ_{11} will less than 1.

A. Role of different types of coherence

Equation (13) above, written in the form of a series, gives a glimpse of the role of the different terms due to TOC. The TOC between level $|1\rangle$ and any general level $|i\rangle$ is ρ_{1i}, as shown in Fig. 1, and corresponds to the term $\frac{1}{4}\frac{\Omega_{i-1i}^2}{\gamma_{1i-1}\gamma_{1i}}$. The first term $\frac{i}{2}\frac{\Omega_{12}}{\gamma_{12}}\rho_{11}$ is the absorption of the probe laser in the absence of any control laser. The TOC between levels $|1\rangle$ and $|3\rangle$, i.e., ρ_{13}, corresponds to the term $\frac{1}{4}\frac{\Omega_{23}^2}{\gamma_{12}\gamma_{13}}$ and causes reduction of the absorption of the probe laser, which is known as EIT. The ρ_{14} corresponding to the term $\frac{1}{4}\frac{\Omega_{34}^2}{\gamma_{13}\gamma_{14}}$ causes induced absorption against the EIT and is known as an EITA. The ρ_{15} corresponding to $\frac{1}{4}\frac{\Omega_{45}^2}{\gamma_{14}\gamma_{15}}$ again reduces the absorption (EITAT), ρ_{16} corresponding to $\frac{1}{4}\frac{\Omega_{56}^2}{\gamma_{15}\gamma_{16}}$ causes increased absorption (EITATA), and so on. The sequence of transparency and absorption can be seen in Λ, N, M, and NN systems, which are described in the next section.

B. Various types of systems

The normalized absorption of the probe laser, i.e., the imaginary part of normalized ρ_{12} for the various systems, is plotted in Fig. 2. The normalized ρ_{12} $(= \frac{\Gamma_1+\Gamma_2}{\Omega_{12}}\rho_{12})$ is such that, for the *stationary atoms* and in the absence of all the control lasers, the maximum absorption of the probe laser is 1. In these plots Γ is taken to be $2\pi \times 6$ MHz. The decoherence rate between the ground states $|1\rangle$ and $|3\rangle$ and $|1\rangle$ and $|5\rangle$, i.e., $\frac{\Gamma_1+\Gamma_3}{2}$ and $\frac{\Gamma_1+\Gamma_5}{2}$, is taken to be $2\pi \times 500$ kHz. This decoherence rate includes collisions and the typical linewidth of the lasers.

First we discuss the three-level Λ system. For this system we truncate the generalized Eq. (13) up to $N = 3$, which

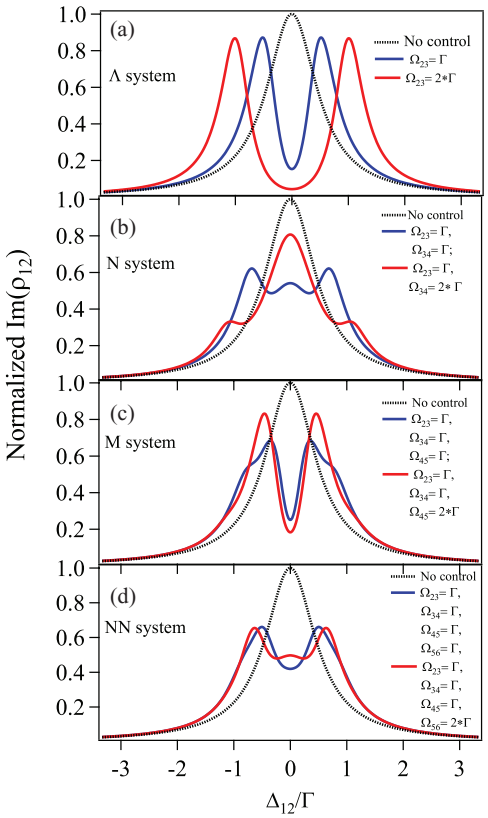

FIG. 2. (Color online) The normalized absorption profile of the probe laser, normalized $\mathrm{Im}(\rho_{12})$ with detuning of the same with different combinations of control lasers Rabi frequencies. The detuning of all the control lasers is zero. The black dotted line indicates the absorption profile of a probe laser in the absence control lasers. The steady state value is $\rho_{11} = 1$.

reduces to the following:

$$\rho_{12} = \frac{\frac{i}{2}\frac{\Omega_{12}}{\gamma_{12}}\rho_{11}}{1 + \frac{1}{4}\frac{|\Omega_{23}|^2}{\gamma_{12}\gamma_{13}}}. \tag{14}$$

The normalized $\mathrm{Im}(\rho_{12})$ of Eq. (14) is plotted in Fig. 2(a). These figures show that at the line center there is a decrease in the absorption of the probe laser in the presence of a control (EIT) and, with the higher value of Ω_{23}, the amplitude and the linewidth of the EIT dip increases. This is well known as the power broadening of EIT.

Now we include one more laser Ω_{34} to form the four-level N system. For this system the general Eq. (13) has to be truncated up to $N = 4$; i.e.,

$$\rho_{12} = \frac{\frac{i}{2}\frac{\Omega_{12}}{\gamma_{12}}\rho_{11}}{1 + \cfrac{\frac{1}{4}\frac{|\Omega_{23}|^2}{\gamma_{12}\gamma_{13}}}{1 + \frac{1}{4}\frac{|\Omega_{34}|^2}{\gamma_{13}\gamma_{14}}}}. \tag{15}$$

The normalized $\mathrm{Im}(\rho_{12})$ of Eq. (15) is plotted Fig. 2(b). This plot shows that in the presence of a control laser, Ω_{34} forming the N system tends to recover the absorption (EITA) against EIT. The recovery of absorption is not complete, because at the line center, the black dotted line shows more absorption as compared to the blue ($\Omega_{34} = \Gamma$) and red traces ($\Omega_{34} = 2\Gamma$).

The reason for the incomplete recovery is the higher decoherence rate between levels $|1\rangle$ and $|4\rangle$ as compared to that between levels $|1\rangle$ and $|3\rangle$, since level $|4\rangle$ is an excited state.

For the five-level M system, Eq. (13) reduces to the following:

$$\rho_{12} = \frac{\frac{i}{2}\frac{\Omega_{12}}{\gamma_{12}}\rho_{11}}{1+\frac{\frac{1}{4}\frac{|\Omega_{23}|^2}{\gamma_{12}\gamma_{13}}}{1+\frac{\frac{1}{4}\frac{|\Omega_{34}|^2}{\gamma_{13}\gamma_{14}}}{1+\frac{1}{4}\frac{|\Omega_{45}|^2}{\gamma_{14}\gamma_{15}}}}}. \tag{16}$$

The normalized $\mathrm{Im}(\rho_{12})$ of Eq. (16) is plotted in Fig. 2(c). In the presence of a control laser (Ω_{45}) which forms the M system, the absorption at the line center of the probe decreases (EITAT), as shown in Fig. 2(c).

For a six-level NN system, Eq. (13) reduces to the following equation:

$$\rho_{12} = \frac{\frac{i}{2}\frac{\Omega_{12}}{\gamma_{12}}\rho_{11}}{1+\frac{\frac{1}{4}\frac{|\Omega_{23}|^2}{\gamma_{12}\gamma_{13}}}{1+\frac{\frac{1}{4}\frac{|\Omega_{34}|^2}{\gamma_{13}\gamma_{14}}}{1+\frac{\frac{1}{4}\frac{|\Omega_{45}|^2}{\gamma_{14}\gamma_{15}}}{1+\frac{1}{4}\frac{|\Omega_{56}|^2}{\gamma_{15}\gamma_{16}}}}}}. \tag{17}$$

In the presence of another control laser (Ω_{56}) which forms an NN system, the absorption tends to recover against transparency (EITATA) but not completely, as shown in Fig. 2(d), due to a higher decoherence rate for ρ_{16} as compared to ρ_{15}, since $|6\rangle$ is an excited state.

C. Mutual influence of the two subsystems

In this section we discuss the case where the strong control lasers of two subsystems share a common level, as shown in Fig. 3. In this figure level $|2\rangle$ is shared by $|1\rangle \rightarrow |2\rangle \leftrightarrow |3\rangle \leftrightarrow \cdots \leftrightarrow |N\rangle$ and $|1\rangle \rightarrow |2\rangle \leftrightarrow |N+1\rangle \leftrightarrow \cdots \leftrightarrow |N+n\rangle$ subsystems. In the weak probe limit case the absorption of the probe is given by

$$\rho_{12} = \frac{\frac{i}{2}\frac{\Omega_{12}}{\gamma_{12}}\rho_{11}}{1+\frac{\frac{1}{4}\frac{|\Omega_{2p}|^2}{\gamma_{12}\gamma_{1p}}}{1+\frac{\cdot}{\cdot}\frac{\cdot}{1+\frac{1}{4}\frac{|\Omega_{N+n-1N+n}|^2}{\gamma_{1N+n-1}\gamma_{1N+n}}}}+\frac{\frac{1}{4}\frac{|\Omega_{23}|^2}{\gamma_{12}\gamma_{13}}}{1+\frac{\cdot}{\cdot}\frac{\cdot}{1+\frac{1}{4}\frac{|\Omega_{N-1N}|^2}{\gamma_{1N-1}\gamma_{1N}}}}}. \tag{18}$$

In deriving the above equation, the procedure and approximation are the same as for Eq. (13).

In support of Eq. (18), we compare this with the complete numerical solution for two special cases. These two cases are also encountered when we discuss the doubly driven Λ system in ^{87}Rb. The first case is an M subsystem, $|1\rangle \rightarrow |2\rangle \leftrightarrow |3\rangle \leftrightarrow |4\rangle \leftrightarrow |5\rangle$, and a Λ subsystem, $|1\rangle \rightarrow |2\rangle \leftrightarrow |N+1\rangle$, sharing common level $|2\rangle$. For this case Eq. (18) reduces to the following:

$$\rho_{12} = \frac{\frac{i}{2}\frac{\Omega_{12}}{\gamma_{12}}\rho_{11}}{1+\frac{1}{4}\frac{|\Omega_{2N+1}|^2}{\gamma_{12}\gamma_{2N+1}}+\frac{\frac{1}{4}\frac{|\Omega_{23}|^2}{\gamma_{12}\gamma_{13}}}{1+\frac{\frac{1}{4}\frac{|\Omega_{34}|^2}{\gamma_{13}\gamma_{14}}}{1+\frac{1}{4}\frac{|\Omega_{34}|^2}{\gamma_{14}\gamma_{15}}}}}. \tag{19}$$

For this case the comparison between numerical and analytical solutions is done in Fig. 4(a).

The second case involves two N subsystems, $|1\rangle \rightarrow |2\rangle \leftrightarrow |3\rangle \leftrightarrow |4\rangle$ and $|1\rangle \rightarrow |2\rangle \leftrightarrow |N+1\rangle \leftrightarrow |N+2\rangle$, sharing the level $|2\rangle$. For this case, Eq. (18) reduces to the following:

$$\rho_{12} = \frac{\frac{i}{2}\frac{\Omega_{12}}{\gamma_{12}}\rho_{11}}{1+\frac{\frac{1}{4}\frac{|\Omega_{2N+1}|^2}{\gamma_{12}\gamma_{1N+1}}}{1+\frac{1}{4}\frac{|\Omega_{N+1N+2}|^2}{\gamma_{1N+1}\gamma_{1N+2}}}+\frac{\frac{1}{4}\frac{|\Omega_{23}|^2}{\gamma_{12}\gamma_{13}}}{1+\frac{1}{4}\frac{|\Omega_{34}|^2}{\gamma_{13}\gamma_{14}}}}. \tag{20}$$

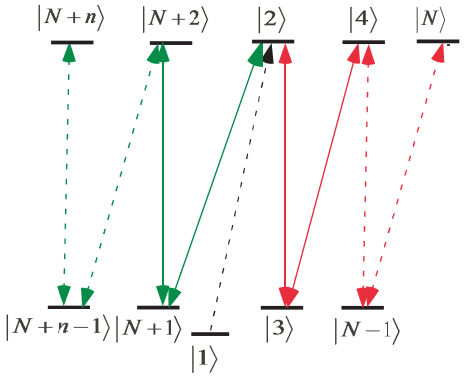

FIG. 3. (Color online) The energy-level diagram of two subsystems sharing common level $|2\rangle$. The dotted black arrow is the probe laser. The control lasers shown by red arrows form one subsystem while control lasers shown with green arrows form another.

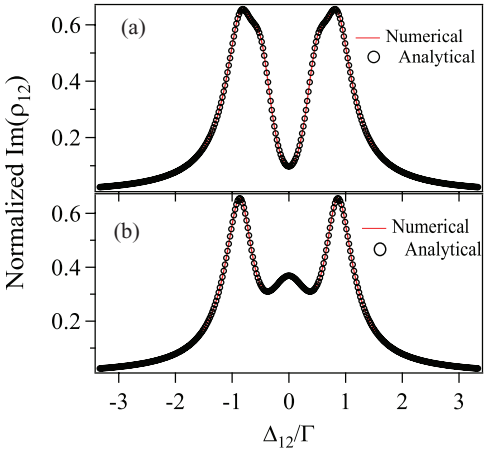

FIG. 4. (Color online) Comparison between numerical and analytical solutions for the imaginary part of normalized ρ_{12} in the presence of control lasers having Rabi frequency Γ ($2\pi \times 6$ MHz). The decoherence rates between ground states is $(1/12)\Gamma$ ($2\pi \times 500$ KHz) (a) forming one Λ system and one M system and (b) forming two N systems.

For this case the comparison between numerical and analytical solutions is done in Fig. 4(b).

D. Effect of the Doppler broadening

The effect of Doppler averaging gives interesting modifications of the line shape of the probe absorption in EIT [3,12,32,33]. Linewidth narrowing up to the subnatural is a quite interesting aspect of it [12,32]. Here we extend this discussion for four-level and beyond-four-level systems of type N, M, and NN.

Doppler broadening arises from the fact that moving atoms with velocity $\vec{v}$ see Doppler shift in the laser frequencies by $\vec{k}\cdot\vec{v}$, where $\vec{k}$ is the wave vector of the laser. The γ_{1j}, which appears in the expression for ρ_{12}, has to be modified by the Doppler shift as

$$\gamma_{1j} = \frac{\Gamma_1+\Gamma_j}{2} - i\sum_{i=1}^{j-1}(-1)^{i+1}(\Delta_{i,i+1} + \vec{k}_{i,i+1}\cdot\vec{v}), \quad (21)$$

where $\vec{k}_{i,i+1}$ is the wave vector of laser $\Omega_{i,i+1}$.

The velocity probability distribution of atoms having mass M at temperature T is given as

$$P(v) = \sqrt{\frac{M}{2\pi k_B T}}\exp\left(\frac{-Mv^2}{2k_B T}\right),$$

where k_B is the Boltzmann constant.

The Doppler averaging of ρ_{12} is given as

$$\int_{-\infty}^{\infty}\rho_{12}(v)P(v)\,dv. \quad (22)$$

Doppler averaging in this work is done numerically for room temperature ($T = 298$ K) for Rb ($M = 87$ amu). The lower and upper limits of the above integral are taken to be -500 and 500 m/s. The probability of an atom having a velocity of more than 500 m/s is very small at room temperature. The Doppler width for Rb at a wavelength of 780 nm at room temperature is around $2\pi/\lambda \times 2\sqrt{(2k_BT)/(M)} \approx 2\pi \times 600$ MHz.

Now we discuss the effect of Doppler broadening for Λ, N, M, and NN systems. For these systems, there exist many configurations for the propagation direction of the various control lasers with respect to a probe laser. But we restrict ourselves to the configurations in the sequence of copropagation and counterpropagation. For example, Ω_{23} is copropagating, Ω_{34} is counterpropagating, Ω_{45} is copropagating, and Ω_{56} is counterpropagating to the probe laser (Ω_{12}). The configurations are shown in the annotations in Fig. 5. This is the configuration which also exists for the subsystems for the doubly driven Λ system in ^{87}Rb and is discussed in the next section. We also consider $|\vec{k}_{12}| = |\vec{k}_{23}| = |\vec{k}_{34}| \cdots = k$, since the wavelength of the lasers for the Λ system in ^{87}Rb is the same ($\approx$780 nm). The imaginary part of normalized ρ_{12}, $(\frac{\Gamma_1+\Gamma_2}{\Omega_{12}\rho_{11}}\rho_{12})$ with Doppler averaging for these systems, is plotted in Fig. 5. The absorption for a Doppler-broadened medium is reduced as compared to stationary atoms by a factor of natural linewidth ($2\pi \times 6$ MHz)/Doppler width ($2\pi \times 600$ MHz) $= 100$.

First we discuss the effect of Doppler broadening for the three-level Λ system. The ρ_{12} for this system involves

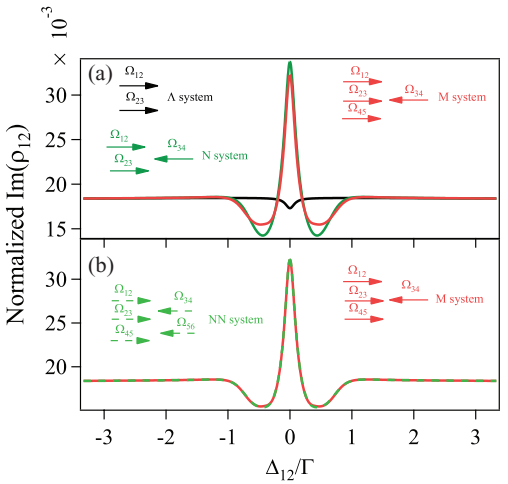

FIG. 5. (Color online) Imaginary part normalized ρ_{12} after Doppler averaging for the various types of system with detuning of the probe laser. The Rabi frequencies of the control lasers are Γ. The detuning of all the control lasers is zero. The propagation direction of individual lasers is shown with arrows in the annotation.

coherence ρ_{13} corresponding to the term $\frac{1}{4}\frac{|\Omega_{23}|^2}{\gamma_{12}\gamma_{13}}$. For moving atoms with velocity v along or opposite to Ω_{12}, the term γ_{12} which includes only probe detuning (Δ_{12}) is modified as $\frac{\Gamma_1+\Gamma_2}{2} - i(\Delta_{12} \pm kv)$. For the case of copropagating Ω_{23} with respect to Ω_{12}, for the γ_{13} which involves two-photon detuning ($\Delta_{12} - \Delta_{23}$), the Doppler effect is zero. The line shape after Doppler averaging for the Λ system is shown in Fig. 5(a). Doppler averaging decreases the amplitude as well as the linewidth of the EIT dip as compared to a stationary atom. The decrease of amplitude and linewidth of the EIT dip has already been studied previously [3,12,32]. In the case of counterpropagating Ω_{23} to Ω_{12}, the two-photon resonance condition is not satisfied for the moving atoms and EIT is washed out by Doppler averaging.

Now we discuss the effect of Doppler broadening for the case of a four-level N system. The N system involves coherence ρ_{14} corresponding to the term $\frac{1}{4}\frac{|\Omega_{34}|^2}{\gamma_{13}\gamma_{14}}$. The term corresponding to ρ_{14} is in the denominator of the term corresponding to ρ_{13}. In order to see the effect of ρ_{14}, the ρ_{13} should survive after Doppler averaging, meaning the two-photon resonance condition should be satisfied. Hence, for the N system, the lasers Ω_{23} should be copropagating to Ω_{12}. This argument is also true for the M and NN systems or any systems in the sequence, since the coherence terms for these systems, i.e., ρ_{15} and ρ_{16}, are in the denominator of ρ_{13}. The N system also involves the three-photon detuning ($\Delta_{12} - \Delta_{23} + \Delta_{34}$) (through γ_{14}). But it is not possible to satisfy the two-photon as well as the three-photon resonance condition for the moving atoms. We consider the configuration with Ω_{23} copropagating and Ω_{34} counterpropagating to Ω_{12}. For atoms moving with velocity v along or opposite to Ω_{12}, the three-photon detuning will be $\Delta_{12} - \Delta_{23} + \Delta_{34} \pm kv$. The line shape of the probe laser after Doppler averaging shows narrow absorption, as shown by the green curve in Fig. 5(a). We saw in the previous subsection that without Doppler averaging in the presence of a control laser Ω_{34} the absorption tends to recover against EIT but not fully [Fig. 2(b)]. The interesting

point is that the counterpropagating Ω_{34} control laser gives maximal effect (EITA) of ρ_{14} even though the three-photon resonance condition is not satisfied for moving atoms.

The M system involves coherence ρ_{15} corresponding to the term $\frac{1}{4}\frac{|\Omega_{45}|^2}{\gamma_{14}\gamma_{15}}$ and contains four-photon detuning. For atoms moving with velocity v along or opposite to Ω_{12}, the four-photon detuning will be $\Delta_{12}-\Delta_{23}+\Delta_{34}-\Delta_{45}\pm 2kv$ for the configuration as shown in the annotation of Fig. 5. After Doppler averaging, the profile for the absorption decreases a little bit [compare the green and red curves in Fig. 5(a)]. The effect of the M system (EITAT) is not maximal since the four-photon resonance condition is not satisfied for the moving atoms.

The NN system involves coherence ρ_{16} corresponding to the term $\frac{1}{4}\frac{|\Omega_{56}|^2}{\gamma_{15}\gamma_{16}}$ and contains five-photon detuning. For atoms moving with velocity v along or opposite to Ω_{12}, the five-photon detuning will be $\Delta_{12}-\Delta_{23}+\Delta_{34}-\Delta_{45}+\Delta_{56}\pm 3kv$ for the configuration as shown in the annotation of Fig. 5. After Doppler averaging the absorption profile shows not much change as compared to the M system, as shown by the green dotted curve and the red curve in Fig. 5(b). This is because the five-photon resonance condition is mismatched by a major amount of $3kv$ for the moving atoms.

In order to see the effect of coherence induced by the control lasers, the two-photon resonance condition (i.e., copropagation of Ω_{23} with respect to Ω_{12}) is an essential condition for the Doppler-broadened medium. Any kind of system which does not satisfy the two-photon resonance condition behaves as the two-level system.

In the case where two subsystems share a common energy level, the Doppler averaging follows the above discussion. In order to see the effect of both subsystems, both have to satisfy the two-photon resonance condition; i.e., $\Delta_{12}-\Delta_{23}=0$ and $\Delta_{12}-\Delta_{2N+1}=0$.

III. VARIOUS SUBSYSTEMS FORMED

We consider the doubly driven Λ system in ^{87}Rb that involves the two ground hyperfine states $F_g=1$ and $F_g=2$ of $5S_{1/2}$ and one excited hyperfine state $F_e=2$ of $5P_{3/2}$. The probe laser drives the $F_g=1\rightarrow F_e=2$ transition and is σ^- polarized. Out of the two control lasers driving $F_g=2\leftrightarrow F_e=2$, one is copropagating and the other is counterpropagating to the probe laser. This problem is analyzed for the following two configurations: (a) with the copropagating control laser having σ^+ polarization and the counterpropagating control laser having σ^- polarization as shown in Figs. 6(a), and 6(b) with the copropagating control laser having σ^- polarization and the counterpropagating control laser having σ^+ polarization as shown in Fig. 6(b). All the states of this doubly driven Λ system are shown in Fig. 6.

The time evolution of the population of the ground states for two combinations of Rabi frequencies of the two control lasers σ^- and σ^+ is shown in Fig. 7. At time $t=0$ at room temperature all the eight ground states are equally populated (1/8). The steady-state population of the ground states $|1\rangle$, $|2\rangle$, and $|3\rangle$ is a maximum. Some of the population is left in states $|4\rangle$, $|8\rangle$, and $|6\rangle$, while the population of states $|5\rangle$ and $|7\rangle$ is almost pumped out.

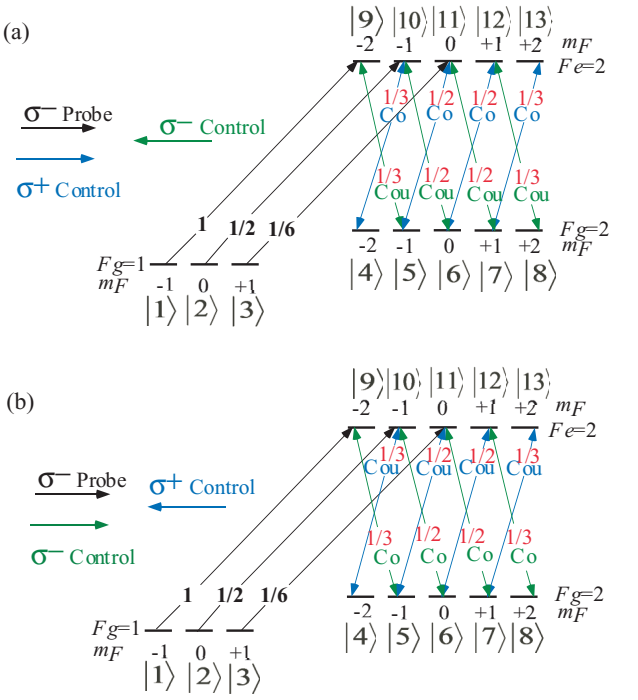

FIG. 6. (Color online) The energy-level diagram for the doubly driven Λ system in ^{87}Rb. The probe laser is σ^- polarized and shown with a black arrow. (a) Control laser which is copropagating (Co) to the probe laser is σ^+ polarized, and counterpropagating (Cou) control laser is σ^- polarized. (b) Control laser which is copropagating (Co) to the probe laser is σ^- polarized and counterpropagating (Cou) control laser is σ^+ polarized.

Figures 6(a) and 6(b) show various subsystems formed by these two counterpropagating control lasers. The probe laser driving $|1\rangle\rightarrow|9\rangle$ forms the NN system; i.e., $|1\rangle\rightarrow|9\rangle$

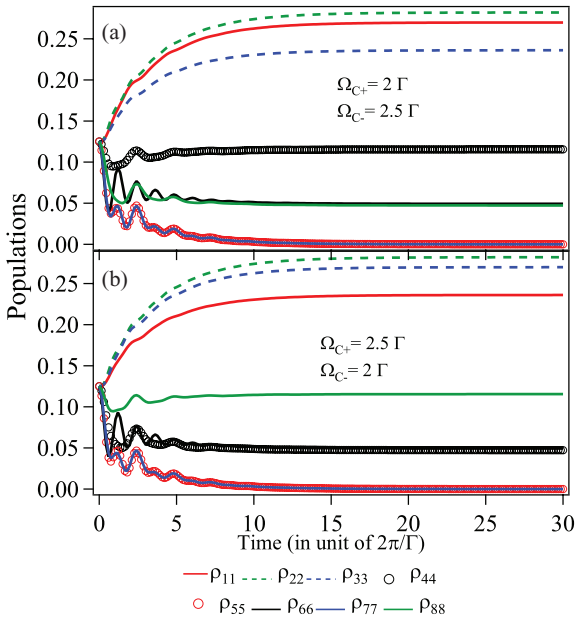

FIG. 7. (Color online) Population evolution of ground states in the presence of σ^+ and σ^- control lasers. (a) The Rabi frequencies of σ^+ and σ^- control lasers are 2Γ and 2.5Γ. (b) The Rabi frequencies of σ^+ and σ^- control lasers are 2.5Γ and 2Γ.

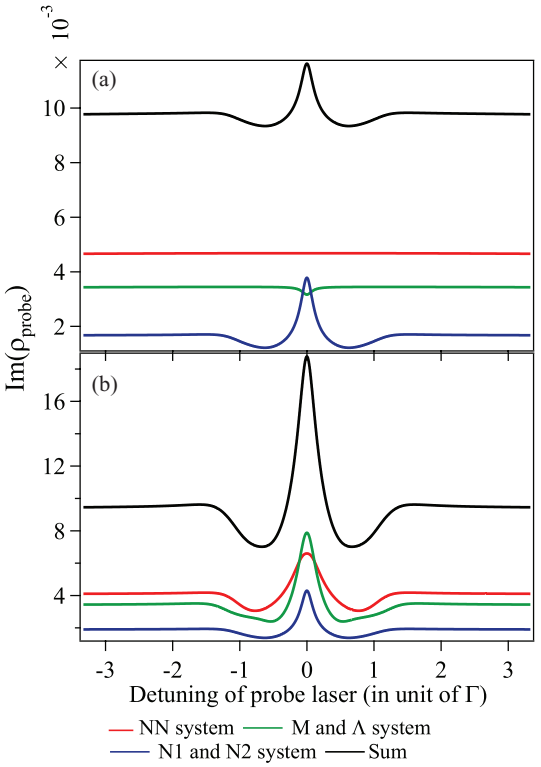

FIG. 8. (Color online) Absorption profile of probes for the various subsystems. Probe is σ^- polarized: (a) σ^+ control laser is copropagating while σ^- control laser is counterpropagating to the probe laser, and (b) σ^- control laser is copropagating while σ^+ control laser is counterpropagating. The Rabi frequency of the copropagating control laser is $2\pi \times 12$ MHz (2 Γ) and of counterpropagating laser is $2\pi \times 15$ MHz (2.5 Γ). The red, green, and blue curves are weighted by the steady-state population of states $|1\rangle$, $|2\rangle$, and $|3\rangle$ and by the Clebsch-Gordan coefficient between $|1\rangle$ and $|9\rangle$ (1), $|2\rangle$ and $|10\rangle$ (1/2), and $|3\rangle$ and $|11\rangle$ (1/6), respectively.

$\leftrightarrow |5\rangle \leftrightarrow |11\rangle \leftrightarrow |7\rangle \leftrightarrow |13\rangle$. The probe laser driving $|2\rangle \rightarrow |10\rangle$ forms one Λ system ($|2\rangle \rightarrow |10\rangle \leftrightarrow |4\rangle$) and one M system ($|2\rangle \rightarrow |10\rangle \leftrightarrow |6\rangle \leftrightarrow |12\rangle \leftrightarrow |8\rangle$). This M system and Λ system share a common level, $|10\rangle$. The probe laser driving $|3\rangle \rightarrow |11\rangle$ forms two N systems, $|3\rangle \rightarrow |11\rangle \leftrightarrow |5\rangle \leftrightarrow |9\rangle$ and $|3\rangle \rightarrow |11\rangle \leftrightarrow |7\rangle \leftrightarrow |13\rangle$). These two N systems share the common level $|11\rangle$.

First we discuss the case of a copropagating σ^+ and counterpropagating σ^-control laser as shown in Fig. 6(a). The probe ($|1\rangle \rightarrow |9\rangle$) which forms an NN system does not satisfy the two-photon resonance condition as control laser $|9\rangle \leftrightarrow |5\rangle$ is counterpropagating to the probe and hence will not show the effect of an NN system, as shown by the flat red curve in Fig. 8(a). The probe ($|2\rangle \rightarrow |10\rangle$) involving one M system and one Λ system will have no contribution from the M system since the control laser $|10\rangle \leftrightarrow |6\rangle$ is counterpropagating to the probe. The Λ system shows EIT as $|10\rangle \leftrightarrow |4\rangle$ copropagating to the probe. The combined effect is shown with a green curve in Fig. 8(a). The probe ($|3\rangle \rightarrow |11\rangle$) forms two N systems; only one of them, $|3\rangle \rightarrow |11\rangle \leftrightarrow |5\rangle \leftrightarrow |9\rangle$, satisfies the two-photon resonance condition while the other N system does not. The effect of EITA for this subsystem is shown with a blue curve in Fig. 8(a). The combined absorption profile is shown with a black curve.

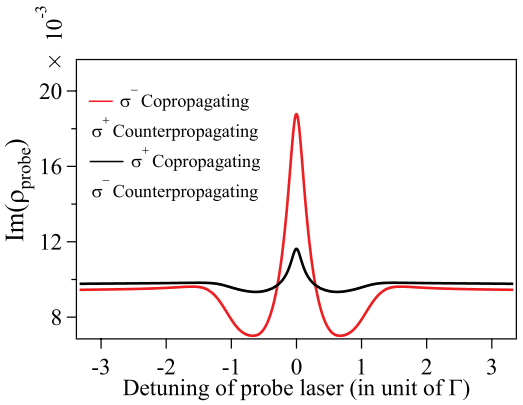

FIG. 9. (Color online) Comparison of the absorption of a probe for two configurations of control laser polarization. The Rabi frequency of the copropagating control laser is $2\pi \times 12$ MHz (2Γ) and that of the counterpropagating laser is $2\pi \times 15$ MHz (2.5Γ).

Now we discuss the case of a copropagating σ^- and counterpropagating σ^+control laser as shown in Fig. 6(b). The probe ($|1\rangle \rightarrow |9\rangle$) which forms an NN system satisfies the two-photon resonance condition and hence shows the EITATA, as shown with a red curve in Fig. 8(b). The probe ($|2\rangle \rightarrow |10\rangle$) forming an M system shows EITAT, while this probe that forms Λ system does not satisfy the two-photon resonance condition and shows no EIT. The absorption profile for this probe is shown with the blue curve in Fig. 8(b). The probe ($|3\rangle \rightarrow |11\rangle$) forms two N systems; only one of them, $|3\rangle \rightarrow |11\rangle \rightarrow |7\rangle \rightarrow |13\rangle$, satisfies the two-photon resonance condition and shows EITA, while the other N system does not satisfy the two-photon resonance condition and will not show EITA. The absorption profile for this probe is shown with a green curve. The combined absorption profile is shown with black curve.

The comparison of absorption profiles for the two configurations is shown in Fig. 9. It is clear that, with the copropagating control laser with σ^- polarization and counterpropagating control laser with σ^+ polarization, the absorption of the probe laser is more as compared to the case with reversed polarizations.

IV. CONCLUSIONS

The general N-level system shows a sequence of EIT and EITA due to the various terms in TOCs. The doubly driven, $F = 1 \rightarrow F = 2 \leftrightarrow F = 2$, Λ system in ^{87}Rb can show the effect of many of these TOC terms depending on the configurations. The σ^+ copropagating and σ^- counterpropagating control laser only shows the effect of the N system, meaning up to ρ_{14}, while σ^- copropagating and σ^+ counterpropagating shows the effect of all N, M, and NN systems, up to ρ_{16}.

ACKNOWLEDGMENTS

We acknowledge Professor Vasant Natarajan and Sapam Ranjita Chanu for important discussions and providing some experimental inputs.

[1] S. E. Harris, J. E. Field, and A. Imamoğlu, Phys. Rev. Lett. **64**, 1107 (1990).
[2] G. S. Agarwal, Phys. Rev. Lett. **67**, 980 (1991).
[3] A. Krishna, K. Pandey, A. Wasan, and V. Natarajan, Europhys. Lett. **72**, 221 (2005).
[4] Shaozheng Jin, Yongqing Li, and Min Xiao, Opt. Commun. **119**, 90 (1995).
[5] A. Imamoğlu and S. E. Harris, Opt. Lett. **14**, 1344 (1989).
[6] K. Pandey, A. Wasan, and V. Natarajan, J. Phys. B **41**, 225503 (2008).
[7] S. Wielandy and Alexander L. Gaeta, Phys. Rev. Lett. **81**, 3359 (1998).
[8] D. F. Phillips, A. Fleischhauer, A. Mair, R. L. Walsworth, and M. D. Lukin, Phys. Rev. Lett. **86**, 783 (2001).
[9] C. Goren, A. D. Wilson-Gordon, M. Rosenbluh, and H. Friedmann, Phys. Rev. A **69**, 053818 (2004).
[10] Y. Zhang, U. Khadka, B. Anderson, and M. Xiao, Phys. Rev. Lett. **102**, 013601 (2009).
[11] R. T. Willis, F. E. Becerra, L. A. Orozco, and S. L. Rolston, Phys. Rev. A **79**, 033814 (2009).
[12] M. G. Bason, A. K. Mohapatra, K. J. Weatherill, and C. S. Adams, J. Phys. B **42**, 075503 (2009).
[13] Tao Hong, Claire Cramer, Warren Nagourney, and E. N. Fortson, Phys. Rev. Lett. **94**, 050801 (2005).
[14] K. Pandey, D. Kaundilya, and V. Natarajan, Opt. Commun. **284**, 252 (2011).
[15] Yi Chen, Xiao Gang Wei, and B. S. Ham, J. Phys. B **42**, 065506 (2009).
[16] D. V. Strekalov, A. B. Matsko, and N. Yu, Phys. Rev. A **76**, 053828 (2007).
[17] S. A. Babin, D. V. Churkin, E. V. Podivilov, V. V. Potapov, and D. A. Shapiro, Phys. Rev. A **67**, 043808 (2003).
[18] C. Affolderbach, S. Knappe, R. Wynands, A. V. Taĭchenachev, and V. I. Yudin, Phys. Rev. A **65**, 043810 (2002).
[19] A. M. Akulshin, S. Barreiro, and A. Lezama, Phys. Rev. A **57**, 2996 (1998).
[20] A. Lezama, S. Barreiro, A. Lipsich, and A. M. Akulshin, Phys. Rev. A **61**, 013801 (1999).
[21] C. Andreeva, S. Cartaleva, Y. Dancheva, V. Biancalana, A. Burchianti, C. Marinelli, E. Mariotti, L. Moi, and K. Nasyrov, Phys. Rev. A **66**, 012502 (2002).
[22] C. Goren, A. D. Wilson-Gordon, M. Rosenbluh, and H. Friedmann, Phys. Rev. A **67**, 033807 (2003).
[23] Sapam Ranjita Chanu, Alok K. Singh, Boris Brun, K. Pandey, and V. Natarajan, Opt. Commun. **284**, 4957 (2011).
[24] Bo Wang, Yanxu Han, Jintao Xiao, Xudong Yang, Changde Xie, Hai Wang, and Min Xiao, Opt. Lett. **31**, 3647 (2006).
[25] Ying-Cheng Chen, Chung-Wei Lin, and Ite A. Yu, Phys. Rev. A **61**, 053805 (2000).
[26] S. R. de Echaniz, A. D. Greentree, A. V. Durrant, D. M. Segal, J. P. Marangos, and J. A. Vaccaro, Phys. Rev. A **64**, 013812 (2001).
[27] O. S. Mishina, M. Scherman, P. Lombardi, J. Ortalo, D. Felinto, A. S. Sheremet, A. Bramati, D. V. Kupriyanov, J. Laurat, and E. Giacobino, Phys. Rev. A **83**, 053809 (2011).
[28] Xiao-Gang Wei, Jin-Hui Wu, Gui-Xia Sun, Zhuang Shao, Zhi-Hui Kang, Yun Jiang, and Jin-Yue Gao, Phys. Rev. A **72**, 023806 (2005).
[29] S. M. Iftiquar and V. Natarajan, Phys. Rev. A **79**, 013808 (2009).
[30] S. R. Chanu, K. Pandey, and V. Natarajan, Europhys. Lett. **98**, 44009 (2012).
[31] M. Suhail Zubairy and Marlan O. Scully, in *Quantum Optics* (Cambridge University Press, Cambridge, 1997), p. 226.
[32] S. M. Iftiquar, G. R. Karve, and V. Natarajan, Phys. Rev. A **77**, 063807 (2008).
[33] K. Pandey and V. Natarajan, J. Phys. B **41**, 185504 (2008).